

## Supplemental material

### Supplemental Methods

#### Genotyping and linkage analysis

Genomic DNA was isolated from lymphoblastoid cell lines or whole-blood samples, by phenol/chloroform extraction. The seven members of this French family affected by a T-cell deficit and persistent EV-HPV infections were genotyped with the Affymetrix Genome-wide SNP 6.0 array. Genotype calling was achieved with Affymetrix Power Tools ([http://www.affymetrix.com/partners\\_programs/programs/developer/tools/powertools.affx](http://www.affymetrix.com/partners_programs/programs/developer/tools/powertools.affx)) for the seven family members, and for an additional sample of 200 individuals genotyped by the same platform, to improve the detection of genotype clusters. Relationships between members of the family affected by a T-cell deficit and persistent EV-HPV infections were confirmed by IBS calculation, with PLINK (1). We discarded monomorphic SNPs, SNPs with a call rate lower than 100% and SNPs presenting Mendelian inconsistencies in the family. SNPs were further filtered with population-based filters. We excluded SNPs displaying more than one Mendelian inconsistency. We then used about 94,000 high-quality SNP markers to carry out linkage analysis, assuming autosomal-recessive inheritance with complete penetrance. Parametric multipoint linkage analysis was carried out with the Merlin program (2). The French family founders and HapMap CEU trios were used to estimate allele frequencies and to define linkage clusters, with an  $r^2$  threshold of 0.4. We searched for homozygous deletions in patients, with PennCNV-joint (3), correcting for waviness. Within linkage regions, patients presented no homozygous deletion encompassing known coding genes that were absent from the DGV database (<http://projects.tcag.ca/variation/>) (data not shown).

### Sequencing

Polymerase chain reaction (PCR) was carried out with *Taq* polymerase (Invitrogen) and the GeneAmp PCR System 9700 (Applied Biosystems). The exons and flanking intron regions of *RHOH* were amplified by PCR from gDNA extracted from patients' EBV-transformed B cells and SV40-transformed fibroblasts. Primer sequences are indicated in Supplemental Table 9. The PCR products were purified by centrifugation through Sephadex G-50 Superfine resin (Amersham Biosciences) and sequenced with the BigDye Terminator cycle sequencing kit (Applied Biosystems). Sequencing products were purified by centrifugation through Sephadex G-50 Superfine resin and sequences were analyzed with a 3730 DNA Analyzer (Applied Biosystems). The known *RHOH* genomic sequences from NCBI (<http://www.ncbi.nlm.nih.gov/gene?term=rhoh>) were aligned with the Seqman alignment program.

### Cell lines and transfection

Peripheral blood mononuclear cells (PBMC) were transformed with *H. saimiri* strain C488, as previously described, to ensure continuous growth (4). Cells were suspended in lymphocyte growth medium (LGM) without IL-2 at a density of  $0.7-1 \times 10^6$  cells/ml and activated by incubation with 1  $\mu$ g/ml phytohemagglutinin (PHA) for 40 to 60 hours. We then added IL-2 (10 to 100 U/ml) and incubated the cells overnight. Infectious HVS C488 virus supernatant ( $\sim 1/10$  vol of culture) was added to  $3-5 \times 10^6$  cells in 25-cm<sup>2</sup> flasks. The source of the infectious virus was the supernatants of cultures of a lytically infected owl monkey kidney cell line (ATCC #CRL-1556). Inoculated cells were kept in LGM without IL-2 for 7 days after infection and were then transferred to LGM supplemented with IL-2. Transformed cells were

cultured in Panserin/RPMI 1640 (ratio 1:1) supplemented with 20% FBS, 1 x Glutamax, 100 U/ml penicillin, 100 U/ml streptomycin, 20 U/ml human rIL-2, at 37°C, under an atmosphere containing 5% CO<sub>2</sub>.

### Antibodies

The anti-CD3 mAb OKT3 (IgG2a) has been described elsewhere (5). The polyclonal rabbit RhoH (A) antibody recognizes an N-terminal epitope (CTSETFPEAYKPTVYENTG) upstream from the mutation found in the patients. Horseradish peroxidase-conjugated anti-rabbit IgG antibody was purchased from Cell Signaling Technology (7074). Immunologic analysis of the T-, B-, and NK cell compartments on whole blood samples was performed by flow cytometry with monoclonal antibodies against CD3, CD4, CD8, CD19, CD16, CD45RA, CD45RO and CD31 (Becton Dickinson), as described elsewhere (6, 7),(8). B-cell subsets were identified on the basis of differential expression of CD10 and CD27 (transitional: CD10<sup>+</sup>CD27<sup>-</sup>; naive: CD10<sup>-</sup>CD27<sup>-</sup>; memory: CD10<sup>-</sup>CD27<sup>+</sup>) as previously described (9). Expression of IgM, IgG and IgA on these B-cell subsets was determined as previously described (9, 10). NKT cells were identified as CD3<sup>+</sup> cells coexpressing the V $\alpha$ 24 and V $\beta$ 11 TCR chains (11). Flow cytometry experiments on cryopreserved PBMCs were carried out with allophycocyanin (APC)-, fluorescein isothiocyanate (FITC)-, phycoerythrin (PE)-, PE-cyanine dye7 (Cy7)-, APC-Cy7-, peridinin-chlorophyll proteins (PercP)-Cy5.5-, Pacific Blue (PB)-, and eFluor450-conjugated antibodies. Immunologic analysis of naive and memory T-cell subsets was performed with the following antibodies: CD4-PE-Cy7 (BD Pharmingen, SK3), CD8-APC (Caltag, 3B5), CD8-PB (BD Pharmingen, RPA-T8), CD45RA-PercP-Cy5.5 (eBioscience, San Diego, CA HI100), CCR7-FITC (R&D systems, 150503), CD127-eFluor450 (eBioscience, eBioRDR5), 2B4-PE

(Beckman Coulter, c1.7), CX3CR1-APC (BioLegend, San Diego, CA, 2A9-1), CD57-PE (BioLegend, HCD57), CD27-APC (eBioscience, O323), CD62L-PE (Caltag, Dreg-56), granzyme B-APC (Caltag, GB11), perforin-PE (eBioscience, dG9). Immunologic analysis of tissue-homing subsets was performed with the following antibodies: the BD Horizon V450-conjugated anti-CD3 antibody (BD, Biosciences, UCHT1) was used for the gating of CD3<sup>+</sup> cells; CD4-APC-Cy7 (Biolegend, OKT4), CD4-APC (Biolegend, RPA-T4), CD8-PercPcy5.5 (Biolegend, SK1), CD8-PE-Cy7 (Biolegend, SK1),  $\alpha$ E (CD103)-PE (Biolegend, Ber-ACT8),  $\alpha$ 4-PE-Cy7 (Biolegend, 9F10), CLA-FITC (MACS, HECA-452),  $\beta$ 7-APC (Biolegend, FIB504),  $\beta$ 7-FITC (Biolegend, FIB504), CCR4-PE (BD, 1G1), CCR6-PE (BD, 11A9), CCR10-PE (R&D Systems, 314305) and mouse IgG1-PE-Cy7 (Biolegend), rat IgG2a-APC (Biolegend). Mouse IgG1-PE (BD), rat IgM-FITC (Biolegend), rat IgG2a-PE (Biolegend) and rat IgG2a-FITC (Biolegend) isotype controls were used to assess the different subsets. Dead cells were excluded with the Aqua Live/Dead marker (Invitrogen, L34957). Finally, the following antibodies were used for the flow cytometry analysis of mouse cells: anti-mouse CD3e-PE or APC (145-2C11), LPAM-1-PE (DATK32), CD49d-FITC (R1-2), CD103-FITC (M290) (all BD), CD45.2-APC-eFluor780 (104) (eBioscience), anti-human/mouse integrin  $\beta$ 7-PE (FIB504) (BioLegend) and anti-human cutaneous lymphocyte antigen-FITC (BD Pharmingen) antibodies. Dead cells were excluded from the analysis by additional staining with 4',6-diamidino-2-phenylindole (DAPI, Sigma-Aldrich).

### RT-qPCR

Total RNA was extracted from *H. saimiri*-transformed T cells in Trizol (Invitrogen). RNA was reverse transcribed directly, with random hexamers and reverse transcriptase (TaqMan

RT reagents, Applied Biosystems). Quantitative PCR was carried out with the 7500 Fast Real-Time PCR system (Applied Biosystems) and the RhoH Taqman gene expression assay probe Hs00180265\_m1. *RHOH* mRNA levels were normalized with respect to the endogenous control, GUS (Hs99999908\_m1, Applied Biosystems).

#### Determination of V $\alpha$ , $\beta$ , $\gamma$ , $\delta$ gene usage and immunoscope analysis

Total RNA was extracted in Trizol (Invitrogen). RNA was reverse transcribed with SuperScript<sup>TM</sup> II Reverse Transcriptase (RT) (Invitrogen), according to the manufacturer's instructions. V $\alpha$ ,  $\beta$ ,  $\gamma$  and  $\delta$  gene usage was determined and immunoscope analysis was performed on cDNA samples, as previously described (12). An aliquot of cDNA was subjected to PCR amplification with each of the 24 TCR V $\beta$  family-specific primers, together with a TCR C $\beta$  primer and a minor groove binder TaqMan probe (Applied Biosystems). Real-time quantitative PCR was conducted in an ABI7300 device (Applied Biosystems). In a second approach, we used 2  $\mu$ l of each of these amplification reactions as a template in run-off reactions with a nested fluorescent primer specific for the C $\beta$  segment. In this reaction, all PCR products were copied into fluorescently labeled single-stranded DNA fragments, irrespective of their TCR J $\beta$  usage or CDR3 sequence. These fluorescent products were separated on an ABI-PRISM 3730 DNA analyzer (Applied Biosystems). The size and intensity of each band were analyzed with Immunoscope software. Fluorescence intensity was plotted in arbitrary units on the  $y$ -axis, whereas the  $x$ -axis corresponds to CDR3 length in amino acids. The Gaussian distribution of the various CDR3 lengths is characteristic of a normal V $\beta$  repertoire. An identical protocol was used to assess the  $\alpha$ ,  $\gamma$  and  $\delta$  chains, with specific primers used for each family.

### Flow cytometry on cryopreserved PBMCs, assessing naive and memory subsets

Cryopreserved PBMCs were thawed in 10% FBS in RPMI and centrifuged for 5 minutes at 4°C and 450 x g. Cells were resuspended in staining buffer (SB: 0.1% BSA, 0.1% sodium azide in PBS) and plated at a density of  $1 \times 10^6$  cells/well in a 96-well V-bottomed plate and various antibodies against human cell surface markers were added. Cells were then incubated in the dark, at 4°C, for 30 minutes, after which they were washed three times with SB. Cells stained only at the surface were fixed in 1% formaldehyde. For additional intracellular staining, cells were resuspended with 2% formaldehyde and incubated at room temperature for 15 minutes. The cells were then washed with SB and resuspended in 0.5% saponin solution (0.5% saponin, 0.1% BSA in PBS) supplemented with either granzyme B or perforin mAbs, and incubated at 4°C for 30 minutes. Cells were then washed three times with 0.5% saponin solution and resuspended in SB. Samples were analyzed on a Canto-II machine (BD).

### **References**

1. Purcell S, Neale B, Todd-Brown K, Thomas L, Ferreira MA, Bender D, et al. PLINK: a tool set for whole-genome association and population-based linkage analyses. *Am J Hum Genet.* 2007 Sep;81(3):559-75.
2. Abecasis GR, Cherny SS, Cookson WO, Cardon LR. Merlin--rapid analysis of dense genetic maps using sparse gene flow trees. *Nat Genet.* 2002 Jan;30(1):97-101.
3. Wang K, Chen Z, Tadesse MG, Glessner J, Grant SF, Hakonarson H, et al. Modeling genetic inheritance of copy number variations. *Nucleic Acids Res.* 2008 Dec;36(21):e138.
4. Fleckenstein B, Ensser A. Herpesvirus saimiri transformation of human T lymphocytes. *Curr Protoc Immunol.* 2004 Nov;Chapter 7:Unit 7 21.
5. Tunnacliffe A, Olsson C, de la Hera A. The majority of human CD3 epitopes are conferred by the epsilon chain. *Int Immunol.* 1989;1(5):546-50.
6. Andre-Schmutz I, Le Deist F, Hacein-Bey-Abina S, Vitetta E, Schindler J, Chedeville G, et al. Immune reconstitution without graft-versus-host disease after haemopoietic stem-cell transplantation: a phase 1/2 study. *Lancet.* 2002 Jul 13;360(9327):130-7.

7. de Saint Basile G, Geissmann F, Flori E, Uring-Lambert B, Soudais C, Cavazzana-Calvo M, et al. Severe combined immunodeficiency caused by deficiency in either the delta or the epsilon subunit of CD3. *J Clin Invest*. 2004 Nov;114(10):1512-7.
8. de Villartay JP, Lim A, Al-Mousa H, Dupont S, Dechanet-Merville J, Coumou-Gatbois E, et al. A novel immunodeficiency associated with hypomorphic RAG1 mutations and CMV infection. *J Clin Invest*. 2005 Nov;115(11):3291-9.
9. Avery DT, Deenick EK, Ma CS, Suryani S, Simpson N, Chew GY, et al. B cell-intrinsic signaling through IL-21 receptor and STAT3 is required for establishing long-lived antibody responses in humans. *J Exp Med*. 2010 Jan 18;207(1):155-71.
10. Ma CS, Hare NJ, Nichols KE, Dupre L, Andolfi G, Roncarolo MG, et al. Impaired humoral immunity in X-linked lymphoproliferative disease is associated with defective IL-10 production by CD4+ T cells. *J Clin Invest*. 2005 Apr;115(4):1049-59.
11. Nichols KE, Hom J, Gong SY, Ganguly A, Ma CS, Cannons JL, et al. Regulation of NKT cell development by SAP, the protein defective in XLP. *Nat Med*. 2005 Mar;11(3):340-5.
12. Lim A, Baron V, Ferradini L, Bonneville M, Kourilsky P, Pannetier C. Combination of MHC-peptide multimer-based T cell sorting with the Immunoscope permits sensitive ex vivo quantitation and follow-up of human CD8+ T cell immune responses. *J Immunol Methods*. 2002 Mar 1;261(1-2):177-94.
13. Kassu A, Tsegaye A, Petros B, Wolday D, Hailu E, Tilahun T, et al. Distribution of lymphocyte subsets in healthy human immunodeficiency virus-negative adult Ethiopians from two geographic locales. *Clin Diagn Lab Immunol*. 2001 Nov;8(6):1171-6.
14. Bisset LR, Lung TL, Kaelin M, Ludwig E, Dubs RW. Reference values for peripheral blood lymphocyte phenotypes applicable to the healthy adult population in Switzerland. *Eur J Haematol*. 2004 Mar;72(3):203-12.
15. Gu Y, Chae HD, Siefring JE, Jasti AC, Hildeman DA, Williams DA. RhoH GTPase recruits and activates Zap70 required for T cell receptor signaling and thymocyte development. *Nat Immunol*. 2006 Nov;7(11):1182-90.
16. Dorn T, Kuhn U, Bungartz G, Stiller S, Bauer M, Ellwart J, et al. RhoH is important for positive thymocyte selection and T-cell receptor signaling. *Blood*. 2007 Mar 15;109(6):2346-55.
17. Porubsky S, Wang S, Kiss E, Dehmel S, Bonrouhi M, Dorn T, et al. RhoH deficiency reduces peripheral T-cell function and attenuates allogeneic transplant rejection. *Eur J Immunol*. 2010 Jan;41(1):76-88.
18. Arnaiz-Villena A, Timon M, Corell A, Perez-Aciego P, Martin-Villa JM, Rigueiro JR. Brief report: primary immunodeficiency caused by mutations in the gene encoding the CD3-gamma subunit of the T-lymphocyte receptor. *N Engl J Med*. 1992 Aug 20;327(8):529-33.
19. Fischer A, de Saint Basile G, Le Deist F. CD3 deficiencies. *Curr Opin Allergy Clin Immunol*. 2005 Dec;5(6):491-5.
20. Recio MJ, Moreno-Pelayo MA, Kilic SS, Guardo AC, Sanal O, Allende LM, et al. Differential biological role of CD3 chains revealed by human immunodeficiencies. *J Immunol*. 2007 Feb 15;178(4):2556-64.
21. Pacheco-Castro A, Alvarez-Zapata D, Serrano-Torres P, Rigueiro JR. Signaling through a CD3 gamma-deficient TCR/CD3 complex in immortalized mature CD4+ and CD8+ T lymphocytes. *J Immunol*. 1998 Sep 15;161(6):3152-60.

22. Morgan NV, Goddard S, Cardno TS, McDonald D, Rahman F, Barge D, et al. Mutation in the TCRalpha subunit constant gene (TRAC) leads to a human immunodeficiency disorder characterized by a lack of TCRalphabeta+ T cells. *J Clin Invest*. 2011 Feb 1;121(2):695-702.
23. Elder ME, Lin D, Clever J, Chan AC, Hope TJ, Weiss A, et al. Human severe combined immunodeficiency due to a defect in ZAP-70, a T cell tyrosine kinase. *Science*. 1994 Jun 10;264(5165):1596-9.
24. Roifman CM, Dadi H, Somech R, Nahum A, Sharfe N. Characterization of zeta-associated protein, 70 kd (ZAP70)-deficient human lymphocytes. *J Allergy Clin Immunol*. 2010 Dec;126(6):1226-33 e1.
25. Katamura K, Tai G, Tachibana T, Yamabe H, Ohmori K, Mayumi M, et al. Existence of activated and memory CD4+ T cells in peripheral blood and their skin infiltration in CD8 deficiency. *Clin Exp Immunol*. 1999 Jan;115(1):124-30.
26. Fischer A, Picard C, Chemin K, Dogniaux S, le Deist F, Hivroz C. ZAP70: a master regulator of adaptive immunity. *Semin Immunopathol*. 2010 Jun;32(2):107-16.
27. Feske S, Picard C, Fischer A. Immunodeficiency due to mutations in ORAI1 and STIM1. *Clin Immunol*. 2010 May;135(2):169-82.
28. Picard C, McCarl CA, Papolos A, Khalil S, Luthy K, Hivroz C, et al. STIM1 mutation associated with a syndrome of immunodeficiency and autoimmunity. *N Engl J Med*. 2009 May 7;360(19):1971-80.
29. Byun M, Abhyankar A, Lelarge V, Plancoulaine S, Palanduz A, Telhan L, et al. Whole-exome sequencing-based discovery of STIM1 deficiency in a child with fatal classic Kaposi sarcoma. *J Exp Med*. 2010 Oct 25;207(11):2307-12.
30. McCarl CA, Picard C, Khalil S, Kawasaki T, Rother J, Papolos A, et al. ORAI1 deficiency and lack of store-operated Ca<sup>2+</sup> entry cause immunodeficiency, myopathy, and ectodermal dysplasia. *J Allergy Clin Immunol*. 2009 Dec;124(6):1311-8 e7.
31. Li FY, Chaigne-Delalande B, Kanellopoulou C, Davis JC, Matthews HF, Douek DC, et al. Second messenger role for Mg<sup>2+</sup> revealed by human T-cell immunodeficiency. *Nature*. 2011 Jul 28;475(7357):471-6.
32. Su HC. Deducator of cytokinesis 8 (DOCK8) deficiency. *Curr Opin Allergy Clin Immunol*. 2010 Dec;10(6):515-20.
33. Randall KL, Chan SS, Ma CS, Fung I, Mei Y, Yabas M, et al. DOCK8 deficiency impairs CD8 T cell survival and function in humans and mice. *J Exp Med*. 2011 Oct 24;208(11):2305-20.
34. Huck K, Feyen O, Niehues T, Ruschendorf F, Hubner N, Laws HJ, et al. Girls homozygous for an IL-2-inducible T cell kinase mutation that leads to protein deficiency develop fatal EBV-associated lymphoproliferation. *J Clin Invest*. 2009 May;119(5):1350-8.
35. Nehme NT, Pachlopnik Schmid J, Debeurme F, Andre-Schmutz I, Lim A, Nitschke P, et al. MST1 mutations in autosomal recessive primary immunodeficiency characterized by defective naive T cells survival. *Blood*. 2011 Dec 14;10.1182/blood-2011-09-378364.

## Supplemental Figure legends

### Supplemental Figure 1

**(A, B)** Histological features of flat wart-like lesions in patients P1 (A) and P2 (B). Haematoxylin Eosin staining of wart sections shows **(A)** perinuclear vacuolization of spinous and granular epidermal cells typical of HPV-3 productively infected cells, or **(B)** enlarged, homogeneously pale-stained, cytoplasm of spinous and granular cells and abundant keratohyaline granules in the upper granular layers typical of EV-HPV productively infected keratinocytes. (original magnification, 40 X)

### **Supplemental Figure 2**

**(A, B, C)** Multipoint linkage analysis for T-cell deficit with persistent EV-HPV infections and chromosomes 2 **(A)**, 4 **(B)** and 11 **(C)**, with a full penetrance model. Only chromosomes including regions with a maximal LOD score are shown. LOD scores (Y axis) are plotted against chromosomal position (cM). The location of *RHOH* is indicated by an arrow.

### **Supplemental Figure 3**

Human RhoH deficiency is not associated with impaired humoral immunity or low percentages of NK and NKT cells. **(A)** Percentages of the various naive and memory B-cell subsets in the CD20<sup>+</sup> B-cell compartment, **(B, C)** Ig-expressing B cells within **(B)** the naive and **(C)** the memory B-cell compartments were assessed by flow cytometry on cryopreserved PBMCs from the two patients (P1 values are indicated by gray squares, P2 values are indicated by gray diamonds) and 8 healthy controls (indicated by black circles). **(D)** NK, **(E)** NKT cell percentages within **(D)** total lymphocytes, **(E)** CD3<sup>+</sup> T cells were assessed by flow cytometry on cryopreserved PBMCs from both patients and 8 healthy controls. Patients' samples were tested twice. There were no significant differences between healthy controls and patients for any of these subsets. Mean values are represented by horizontal bars.

#### Supplemental Figure 4

Human RhoH deficiency is associated with a lack of naive T cells and an excess of effector memory cells in both CD4<sup>+</sup> and CD8<sup>+</sup> populations. The frequencies of **(A, D)** naive (CD45RA<sup>+</sup>CCR7<sup>+</sup>), **(B, E)** central memory (CD45RA<sup>-</sup>CCR7<sup>+</sup>), **(F)** T<sub>EMRA</sub> (CD45RA<sup>+</sup>CCR7<sup>-</sup>) and **(C, G)** T<sub>EM</sub> (CD45RA<sup>-</sup>CCR7<sup>-</sup>) subsets of CD4<sup>+</sup> T cells **(A-C)** and CD8<sup>+</sup> T cells **(D-G)** in the cryopreserved PBMCs of the patients (P1 values indicated by gray squares, P2 values indicated by gray diamonds) and 8 healthy controls (indicated by black circles) were determined by flow cytometry. Patients' samples were tested twice. Mean values are represented by horizontal bars. Similar results were obtained in the two experiments. (\* =  $p < 0.05$ ; \*\* =  $p < 0.005$ ; \*\*\* =  $p < 0.0005$ ; ns = non significant).

#### Supplemental Figure 5

Patients P1 and P2 have abnormal V $\alpha$  $\beta$  and V $\gamma$  $\delta$  distributions. Immunoscope profiles of **(A)** TCR $\alpha$ , **(B)** TCR $\beta$ , **(C)** TCR $\gamma$  **(D)** TCR $\delta$  for cDNAs obtained from the patients and controls following RNA extraction from PBMCs. Only profiles for V $\alpha$ , V $\beta$  and TCR $\gamma$  $\delta$  differing between the two patients and controls are shown, with a more oligoclonal pattern observed in the patients. The  $x$ -axis indicates CDR3 length (number of amino acids) and the  $y$ -axis shows the fluorescence intensity of the run-off products, in arbitrary units. The percentages indicate relative frequency of usage.

#### Supplemental Figure 6

Human RhoH deficiency is associated with an excess of exhausted memory CD4<sup>+</sup> and CD8<sup>+</sup> T cells. Frequencies of T<sub>EM</sub> (CD45RA<sup>-</sup>CCR7<sup>-</sup>) CD4<sup>+</sup> **(A-D)** and CD8<sup>+</sup> **(E-H)** T cells and

frequencies of T<sub>EMRA</sub> CD8<sup>+</sup> T cells (CD45RA<sup>+</sup>CCR7<sup>-</sup>) (**E-H**) for the patients (P1 values indicated by gray squares, P2 values indicated by gray diamonds) and 8 healthy controls (indicated by black circles) expressing CD127 and 2B4 (**A,E**), CD27 and CD62L (**B,F**), CX3CR1 and CD57 (**C,G**), granzyme and perforin (**D,H**). All subsets were assessed by flow cytometry on cryopreserved PBMCs (\* =  $p < 0.05$ ; \*\* =  $p < 0.005$ ; \*\*\* =  $p < 0.0005$ ; ns = non significant). Patients' samples were tested twice. Mean values are represented by horizontal bars. Similar results were obtained in the two experiments.

### **Supplemental Figure 7**

Human RhoH deficiency leads to a severe decrease in the number of peripheral  $\beta 7^+$  T cells, particularly in the CD4<sup>+</sup> T-cell subset. (**A, B, D, E**) Skin-homing CLA<sup>+</sup>CCR4<sup>+</sup>, CLA<sup>+</sup>CCR6<sup>+</sup> and CLA<sup>+</sup>CCR10<sup>+</sup> subsets were assessed by flow cytometry on live CD3<sup>+</sup> CD4<sup>+</sup> and CD3<sup>+</sup> CD8<sup>+</sup> PBMCs from both patients and from 12, 17 and 12 healthy controls, respectively. (**C, F**)  $\alpha E^+$ CLA<sup>+</sup> cells were assessed by flow cytometry on live CD3<sup>+</sup>, CD3<sup>+</sup>CD4<sup>+</sup> and CD3<sup>+</sup>CD8<sup>+</sup> PBMCs from both patients and 23 healthy controls. (**G, H, I, J**)  $\beta 7^+$ ,  $\alpha 4^+$ ,  $\alpha 4^+\beta 7^+$  and  $\alpha 4^+\beta 7^+$  subsets were assessed by flow cytometry on live CD3<sup>+</sup>CD4<sup>+</sup> and CD3<sup>+</sup>CD8<sup>+</sup> PBMCs from both patients and 12 healthy controls. All assays were carried out on cryopreserved PBMCs. The counts of the various subsets are expressed in (**A, B, C, G, H**) frequencies among CD3<sup>+</sup> cells and (**D, E, F, I, J**) counts per one million live PBMCs. P1 values are indicated by gray squares, P2 values are indicated by gray diamonds and healthy control values are indicated by black circles. Viability rates of about 95% were recorded for all PBMC preparations. Patients' samples were tested at least twice, except for the chemokine receptors, which were assessed only once. Mean

values are represented by horizontal bars (\* =  $P < 0.05$ ; \*\* =  $P < 0.005$ ; \*\*\* =  $P < 0.0005$ ; ns = non significant).

### Supplemental Figure 8

Human and mouse RhoH deficiencies lead to an abnormal integrin expression pattern. **(A, B, C, D, E)** Tissue-homing T-cell subsets were assessed on live CD3<sup>+</sup>-gated cryopreserved PBMCs from the two patients (P1 values indicated by gray squares, P2 values indicated by gray diamonds) and healthy controls (indicated by black circles), by flow cytometry **(A)** Skin-homing CLA<sup>+</sup> subsets were assessed on live CD3<sup>+</sup>, CD4<sup>+</sup> and CD8<sup>+</sup> gated PBMCs from both patients and 28 healthy controls. **(B)** CCR4<sup>+</sup>, CCR6<sup>+</sup> and CCR10<sup>+</sup> subsets were assessed for both patients and 12, 17 and 12 healthy controls, respectively. **(C)** Skin-homing CLA<sup>+</sup>CCR4<sup>+</sup>, CLA<sup>+</sup>CCR6<sup>+</sup> and CLA<sup>+</sup>CCR10<sup>+</sup> subsets were assessed for both patients and for 12, 17 and 12 healthy controls, respectively. **(D)**  $\alpha E^+ \beta 7^+$  cells were assessed on live CD3<sup>+</sup>, CD3<sup>+</sup>CD4<sup>+</sup>, CD3<sup>+</sup>CD8<sup>+</sup> gated PBMCs from both patients and 14 healthy controls. **(E)**  $\beta 7^+$ ,  $\alpha 4^+$ ,  $\alpha 4^+ \beta 7^+$  and  $\alpha 4^+ \beta 7^-$  subsets were assessed for both patients and 12 healthy controls. The counts for the various subsets are expressed in counts per one million live PBMCs. Viability rates were about 95% for all PBMC preparations. Patients' samples were tested at least twice, except for the chemokine receptors, which were assessed only once. Mean values are represented by horizontal bars. The values obtained in all experiments were similar. **(F)** Total counts of  $\beta 7^+$ ,  $\alpha 4^+$ ,  $\alpha E^+ \beta 7^+$  and  $\alpha 4^+ \beta 7^+$  cells were assessed by flow cytometry on CD3<sup>+</sup>-gated peripheral blood cells from *RhoH*<sup>+/+</sup> (N=5) and *RhoH*<sup>-/-</sup> mice (mean +/- SEM, n=5 mice of mixed background) (\* =  $p < 0.05$ ; \*\* =  $p < 0.005$ ; \*\*\* =  $p < 0.0005$ , ns = non significant).

### Supplemental Figure 9

RhoH deficiency is associated with an abnormal distribution of CLA and  $\alpha E\beta 7$  expression in the various naive and memory T-cell compartments. **(A, B)** CLA<sup>+</sup> cells were assessed in cryopreserved PBMCs by flow cytometry on **(A)** CD4<sup>+</sup> or **(B)** CD8<sup>+</sup> gated naive and memory subsets, using the CD45RA and CCR7 markers. **(C, D)**  $\alpha E\beta 7$ <sup>+</sup> cells were assessed by flow cytometry on cryopreserved PBMCs on **(C)** CD4<sup>+</sup> or **(D)** CD8<sup>+</sup> gated naive and memory subsets, using the CD45RA and CCR7 markers. Patients' samples were tested twice. Mean values are represented by horizontal bars. (\* =  $p < 0.05$ ; \*\* =  $p < 0.005$ ; \*\*\* =  $p < 0.0005$ ; ns = non significant).

**Supplemental Table 1: List of protein-coding genes in the maximum LOD score region on chromosome 2**

Region 1 (6.1 Mb)		
DNMT3A	ABHD1	GPN1
DTNB	PREB	SUPT7L <sup>A</sup>
ASXL2	C2orf53	SLC4A1AP
KIF3C	TCF23	MRPL33
RAB10 <sup>A</sup>	SLC5A6	RBKS
FAM59B	C2orf28	BRE <sup>A</sup>
HADHA	CAD	FOSL2 <sup>A</sup>
HADHB	SLC30A3 <sup>A</sup>	PLB1 <sup>A</sup>
GPR113	DNAJC5G	PPP1CB <sup>A</sup>
EPT1	TRIM54	SPDYA <sup>A</sup>
CCDC164	UCN <sup>A</sup>	TRMT61B
OTOF	MPV17	WDR43
C2orf70	GTF3C2	FAM179A <sup>c</sup>
CIB4	EIF2B4	C2orf71
KCNK3 <sup>A</sup>	SNX17	CLIP4
C2orf18	ZNF513	ALK
CENPA	PPM1G <sup>A</sup>	YPEL5
DPYSL5	NRBP1	LBH <sup>A</sup>
MAPRE3	KRTCAP3	LCLAT1
TMEM214	IFT172	CAPN13
AGBL5	FNDC4	GALNT14
OST4 <sup>B</sup>	GCKR	CAPN14
EMILIN1	C2orf16	EHD3
KHK	ZNF512 <sup>A</sup>	XDH
CGREF1 <sup>A</sup>	CCDC121 <sup>A</sup>	

<sup>A</sup> covered by WES and Sanger-sequenced

<sup>B</sup> not covered by WES

<sup>C</sup> non reported homozygous frameshift mutation

**Supplemental Table 2: List of protein-coding genes in the maximum LOD score regions on chromosome 4**

Region 1 (3.3 Mb)	Region 2 (4.5 Mb)		Region 3 (10.8 Mb)	
QDPR	TBC1D1	APBB2	UNC5C	DDIT4L
CLRN2	KLF3	UCHL1	PDHA2	EMCN
LAP3	TLR10	LIMCH1	C4orf37	PPP3CA
MED28	TLR1	PHOX2B	RAP1GDS1	BANK1
FAM184B	TLR6	TMEM33	TSPAN5	SLC39A8 <sup>A</sup>
DCAF16	FAM114A1	DCAF4L1	EIF4E	NFKB1
NCAPG	TMEM156	SLC30A9 <sup>A</sup>	METAP1	MANBA
LCORL	KLHL5	BEND4	ADH5	UBE2D3
SLIT2	WDR19	SHISA3	ADH4	CISD2
	RFC1	ATP8A1	ADH6	SLC9B1
	KLB		ADH1A	SLC9B2
	RPL9		ADH1B	BDH2
	LIAS		ADH1C	CENPE
	UGDH		ADH7	TACR3
	C4orf34		C4orf17	CXXC4
	UBE2K		RG9MTD2	TET2
	PDS5A		MTTP	PPA2
	N4BP2		LOC285556 <sup>B</sup>	ARHGEF38
	RHOH <sup>A</sup>		DAPP1	INTS12
	CHRNA9		LAMTOR3	GSTCD
	RBM47		DNAJB14	NPNT
	NSUN7		H2AFZ	

<sup>A</sup> covered by WES and Sanger-sequenced

<sup>B</sup> not covered by WES

**Supplemental Table 3: List of protein-coding genes in the maximum LOD score region on chromosome 11**

---

Region 1 (5.9 Mb)
LUZP2
ANO3
MUC15
SLC5A12
FIBIN
BBOX1
CCDC34
LGR4
LIN7C
BDNF
KIF18A
METT5D1
KCNA4
FSHB
C11orf46
MPPED2

---

**Supplemental Table 4. General immunophenotyping of patients' hematopoietic cells**

	Patient 1 (26-30 years)			Patient 2 (15-20 years)			Normal range
Patient's age	26	29	30	15	18	19	
<i>Lymphocytes</i>							
T cells							
TcR $\gamma\delta$ (%)	5	ND	ND	3	ND	ND	2-13 <sup>C</sup>
B cells							
CD19 <sup>+</sup> (%)	5	4	7	14	5	12	6-17 <sup>B</sup>
<i>NK cells</i>							
CD56 <sup>+</sup> CD3 <sup>+</sup> (%)	2	ND	ND	ND	ND	ND	
CD56 <sup>+</sup> CD3 <sup>-</sup> (%)	4	ND	ND	2	ND	ND	
CD16 <sup>+</sup> CD56 <sup>+</sup> (%)	ND	3	3	ND	2	1	4.2—35.6 <sup>C</sup>
<i>Monocytes (*10<sup>9</sup>/l)</i>	ND	0.9	0.6	ND	0.8	0.6	0.2-1 <sup>C</sup>
<i>Polymorphonuclear neutrophils (*10<sup>9</sup>/l)</i>	ND	7.2	4.4	ND	5.6	5.5	1.5-7 <sup>C</sup>
<i>Polymorphonuclear eosinophils (*10<sup>9</sup>/l)</i>	ND	0.2	0.1	ND	0.1	0	0-0.5 <sup>C</sup>
<i>Polymorphonuclear basophils (*10<sup>9</sup>/l)</i>	ND	0.1	0	ND	0	0	0-0.2 <sup>C</sup>

<sup>A</sup>Normal ranges taken from the work of Kassu *et al.* (13)

<sup>B</sup>Normal ranges taken from the work of Bisset *et al.* (14)

<sup>C</sup>Internal laboratory controls (N=10)

**Supplemental Table 5. Patients' T-cell phenotype, from the analysis of whole-blood samples**

	Patient 1 (26-30 years)			Patient 2 (15-20 years)			Normal range
Patient's age (years)	26	29	30	15	18	20	
Total lymphocyte (counts/ $\mu$ l)	NA	4000	ND	NA	3500	ND	1120-3370 <sup>A</sup>
<i>T cells</i>							
CD3 <sup>+</sup> (%)	90	93	ND	84	93	ND	64-85 <sup>B</sup>
CD4 <sup>+</sup> (%)	28	31	ND	31	27	ND	34-62 <sup>B</sup>
CD8 <sup>+</sup> (%)	58	60	ND	52	64	ND	14-42 <sup>B</sup>
<i>CD4<sup>+</sup> subset</i>							
CD4 <sup>+</sup> CD45RA <sup>+</sup> (%)	16	13	ND	4	11	ND	20-86 <sup>C</sup>
CD4 <sup>+</sup> CD31 <sup>+</sup> CD45RA <sup>+</sup> (%)	2	4	ND	2	2	ND	30-48 <sup>C</sup>
CD4 <sup>+</sup> CD45RO <sup>+</sup> (%)	97	97	ND	96	98	ND	29-63 <sup>C</sup>
<i>CD8<sup>+</sup> Subset</i>							
CD8 <sup>+</sup> CCR7 <sup>+</sup> CD45RA <sup>+</sup> (%)	ND	ND	ND	ND	ND	ND	37-50 <sup>C</sup>
CD8 <sup>+</sup> CCR7 <sup>+</sup> CD45RA <sup>-</sup> (%)	ND	ND	ND	ND	ND	ND	6-16 <sup>C</sup>
CD8 <sup>+</sup> CCR7 <sup>-</sup> CD45RA <sup>-</sup> (%)	ND	ND	ND	ND	ND	ND	24-37 <sup>C</sup>
CD8 <sup>+</sup> CCR7 <sup>-</sup> CD45RA <sup>+</sup> (%)	ND	ND	ND	ND	ND	ND	8-20 <sup>C</sup>
T-cell proliferation <sup>D</sup>							
3-day culture							
PHA	66.8	37	33.4	42.2	46.1	41.4	>50 <sup>C</sup>
OKT3 50 ng/ml	4.6	ND	0.7	5.9	ND	0.25	>30 <sup>C</sup>
OKT3 25 ng/ml	1.8	ND	0.7	2.7	ND	1.0	>30 <sup>C</sup>
OKT3 10 ng/ml	1.4	ND	0.05	0.9	ND	0.0	>30 <sup>C</sup>
PMA (10 <sup>-7</sup> M) + ionomycin (10 <sup>-5</sup> M)	ND	ND	15.4	ND	ND	13.9	>80 <sup>C</sup>
PMA (10 <sup>-8</sup> M) + ionomycin (10 <sup>-6</sup> M)	ND	ND	28.4	ND	ND	36.4	>80 <sup>C</sup>
6-day culture							
Tetanus toxoid	22.2	2.1	7.05	5.5	7.7	3.05	>10 <sup>C</sup>
Tuberculin	ND	9.7	ND	ND	0.5	24.6	>10 <sup>C</sup>
Candidin	2.2	0.7	0.1	2.9	1.7	0.3	>10 <sup>C</sup>
Herpes simplex virus 1	1.5	ND	ND	0.8	ND	ND	>10 <sup>C</sup>

<sup>A</sup>Normal ranges taken from the work of Kassu *et al.* (13)

<sup>B</sup>Normal ranges taken from the work of Bisset *et al.* (14)

<sup>C</sup>Internal laboratory controls (N=10)

**Supplemental Table 6. Humoral immunity of the patients' peripheral blood**

	P1 (9 years)	Age-matched controls	P2 (20 years)	Age-matched controls
<i>Serum Ig (mg/ml)</i>				
IgG	6.11	6.4-12.4	7.07	6.0-11.1
IgG1	3.4	>4	3.5	>4
IgG2	0.4	>0.6	0.9	>0.5
IgG3	2.89	>0.17	0.31	>0.17
IgG4	0.004	-	0.01	-
IgA	11.6	0.8-3.4	1.26	0.49-1.55
IgM	4.79	0.5-1.5	0.97	0.57-1.59
<i>Specific antibodies</i>				
Tetanus	0.11	>0.1	2.61	>0.1
Diphtheria	<0.10	>0.1	1.14	>0.1
<i>S. pneumoniae</i> (µg/ml)	1.1	>0.3	NA	>0.3
<i>H. influenza</i> (inhibition ratio%)	23	10-30	92	10-30
Poliovirus type 1	10	>40	80	>40
Poliovirus type 2	20	>40	>640	>40
Poliovirus type 3	<10	>40	160	>40

**Supplemental Table 7. Comparison of T-cell phenotypes between mouse RhoH deficiency and human RHOH deficiency**

Mouse RhoH deficiency	Human RHOH deficiency
Severe T-cell lymphopenia (15)	Normal total T-cell count
Low CD8/CD4 ratio in lymph nodes and normal ratio in spleen (16)	CD8 lymphocytosis/normal CD4 <sup>+</sup> count
Decreased naive CD4 <sup>+</sup> and CD8 <sup>+</sup> cell numbers (spleen and lymph nodes)	Lack of naive CD4 <sup>+</sup> and CD8 <sup>+</sup> T cells
Increased memory CD4 <sup>+</sup> and CD8 <sup>+</sup> cell numbers (spleen and lymph nodes) (17)	
Impaired calcium influx and proliferation of splenocytes in response to CD3 stimulation (15)	Impaired proliferation of peripheral T cells in response to CD3 stimulation
Impaired proliferation of thymocytes in response to CD3 stimulation (15)	Normal proliferation in response to PHA, CD3/CD28 Abs and PMA/ionomycin
Impaired β-selection and positive selection	Abnormal Vαβ and Vγδ repertoires
Decreased β7 <sup>+</sup> , αE <sup>+</sup> , αEβ7 <sup>+</sup> cell frequencies & total counts	Low β7 <sup>+</sup> cell frequency & total counts

**Supplemental Table 8. Comparison of RHOH deficiency with other PIDs involving T-cell defects**

Genetic etiology <sup>B</sup>	T-cell counts	Naive/memory T-cell phenotype	T-cell response to various stimuli <sup>A</sup>				Clinical phenotype		
			OKT3	PHA	P/I <sup>C</sup>	Recall antigens	Lung disease	Skin disease	Other
RHOH	Total normal, decreased CD4 counts, increased CD8 counts	Naive CD4 and CD8 lymphopenia Exhaustion of memory	Impaired	Positive but value below normal range	Positive but value below normal range	Variable	Unknown etiology	EV, molluscum (P2), HSV-1 (P2)	Burkitt lymphoma
CD3 $\gamma$ (18-21)	Total normal, decreased CD8 counts	Naive CD4 and CD8 lymphopenia	Impaired	Impaired	Normal	Weak	Bacterial and viral infections	-	Diarrhea, Autoimmunity
TCR $\alpha$ (22)	Total normal (all TCR $\gamma\delta$ ), normal CD4, normal CD8	Normal CD45 <sup>+</sup> CD27 <sup>+</sup>	Impaired	Impaired	ND	Normal	Recurrent infections	Candidiasis	Diarrhea, Chronic herpes infections (varicella, EBV, HHV6), Autoimmunity
Zap70 (23-26)	Total normal to high, T CD8 lymphopenia	Decreased naive CD4	Impaired	Impaired	Impaired	Impaired	Recurrent infections (viral, bacterial, fungal)	MCV <sup>c</sup>	Mycobacterial infections, Autoimmunity
STIM1 (27-29)	Normal	Decreased naive CD4 counts	Impaired	Impaired	Impaired	Impaired	Recurrent infections (viral, bacterial)	VZV	Urinary tract infections, herpes infections (HHV8), autoimmunity, ectodermal dysplasia, myopathy
ORAI1 (27, 30)	Normal	Decreased naive CD4 counts, Increased memory CD4 counts, CD8 ND	Impaired	Impaired	Normal to impaired	Normal to impaired	Recurrent infections (viral, bacterial)	CMC <sup>c</sup>	Viral, mycobacterial, bacterial and fungal infections, autoimmunity ectodermal dysplasia, myopathy
MAGT1 (31)	Total normal, decreased CD4 counts	Decreased naive CD4	Impaired <sup>D</sup>	ND	Normal <sup>D</sup>	Variable	Recurrent infections (viral, bacterial)	-	Chronic EBV infection
DOCK8 (32, 33)	Total normal to low, CD4	Naive CD8	Impaired for	ND <sup>c</sup>	ND	Variable	Recurrent infections	Bacterial and viral (MCV)	Severe food and

	and CD8 normal to low	lymphopenia Exhaustion of memory	CD8 and CD4 T cells				(fungal and bacterial)	infections, eczema	environmental allergies; Gastrointestinal infections, malignancies, autoimmunity
ITK (34)	Total number low, decrease in CD4 counts, decrease in CD8 counts, loss of NKT cells	Decreased naive CD4 counts Increased memory cell counts	Impaired	Normal	ND	Impaired	Recurrent infections	-	EBV-Hodgkin lymphoma, viral and bacterial infections, impaired liver function, autoimmunity
MST1 (35)	Progressive CD4 lymphopenia	Low naive CD4 and CD8 counts	Impaired	Impaired	Weak response	Impaired	Recurrent infections (bacterial)	Dermatitis, recurrent infections (HSV1-2, VZV, molluscum contagiosum)	Chronic EBV infections, autoimmunity,

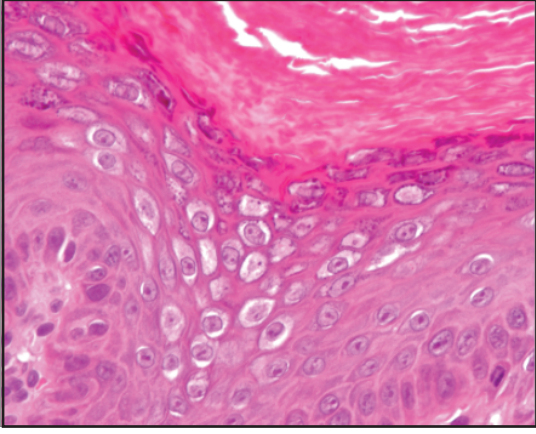
- A: T-cell responses in terms of cell proliferation
- B: CD8 deficiency was not included because of the lack of at least one phenotype common with RHOH deficiency
- C: P/I: PMA + ionomycin, ND: not done, MCV: molluscum contagiosum virus, CMC: mucocutaneous candidiasis, NA: not available
- D: T-cell response in terms of CD69, CD25, Fas (CD95) and CTLA-4 upregulation

### Supplemental Table 9. Primers used to sequence the *RHOH* gene from gDNA samples

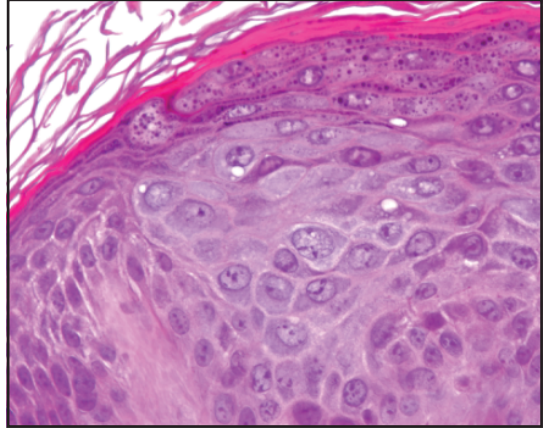
Primer name	Sequence 5'-3'
gRHOHE1F1	CATAGTCTCGGAGTAGGGTG
gRHOHE1R1	ACACCTTACAGCAGGTAGCTC
gRHOHE2F1	CTAAGGCCAGTCTGTTGCATC
gRHOHE2R1	TGCCTCCCGGTCAAGAAGC
gRHOHE3F1	GATCTAAGCTCTCCCTGTGAG
gRHOHE3R1	ACACTCTCTTGCTTCTGTTCC
gRHOHE3F2	GCTGAATGGCGTGTGCTGC
gRHOHE3F3	CAGGCAGACGTGGTGCTG
gRHOHE3F4	AGGAGACGAAACAGAAGGAG
gRHOHE3F5	CCTTGCCCAGGCCAGTTAG
gRHOHE3F6	TCACCTCAAGTAGAAAGTCTG
gRHOHE3R2	CCAGCAGCCAAGTGGTTTC
gRHOHE3R3	GAGTTCACTGTAGAGTGTAG
gRHOHE3R4	GCTGAGCACTCCAGGTAGC
gRHOHE3R5	TAGGCCTCCGGGAAGGTC
gRHOHE3R6	TTCCCGGCCCTCCCTCTC
gRHOHE3R7	GATCTTGCACTCATTGATGG
gRHOHE3F7	GGACGTCTTCATGGATGGC
gRHOHE3F8	GCCTCTGGGACACAGCCG

# Supplemental Figure 1

**A**

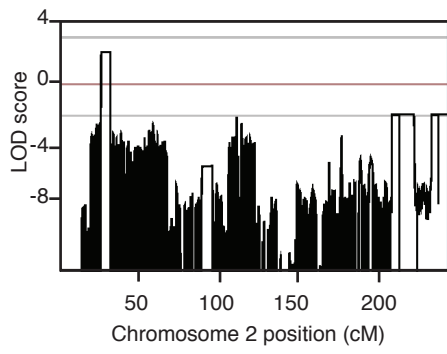


**B**

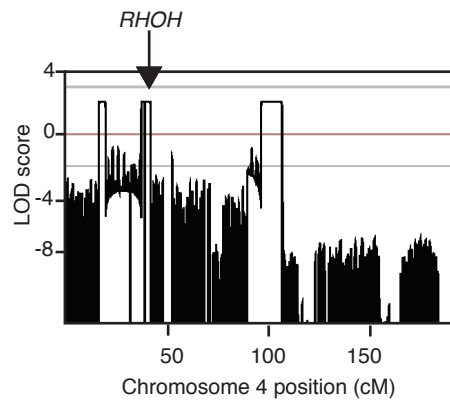


# Supplemental Figure 2

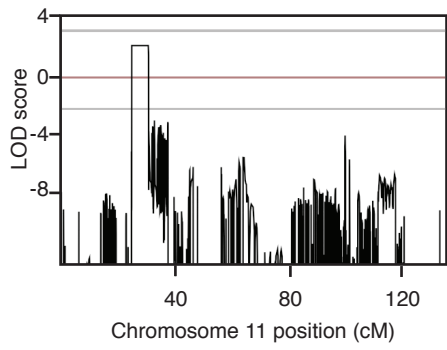
**A**



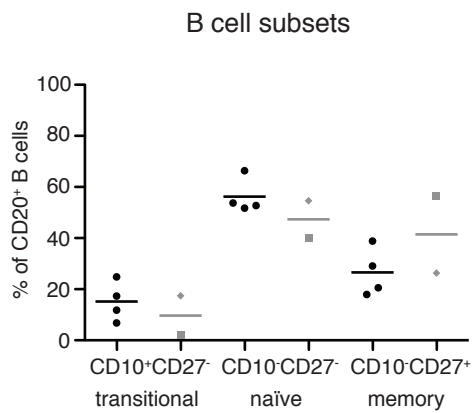
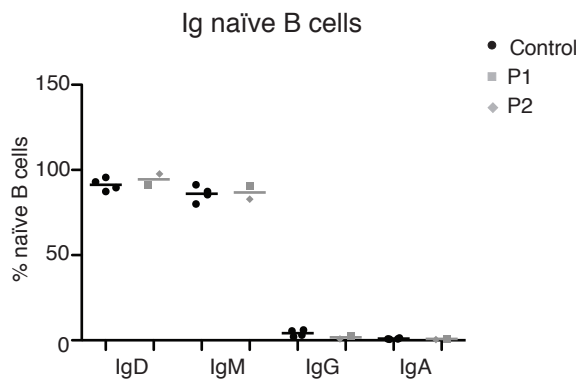
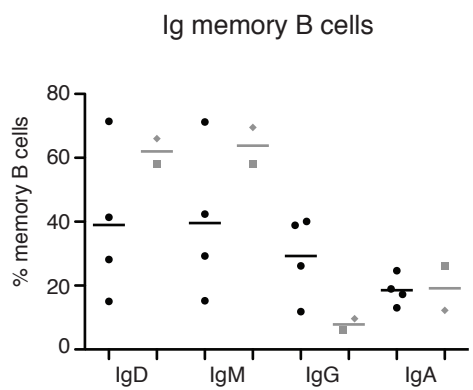
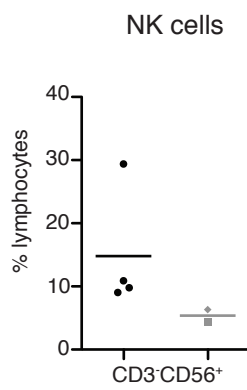
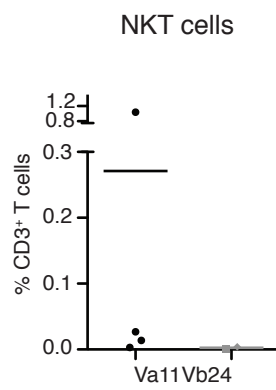
**B**



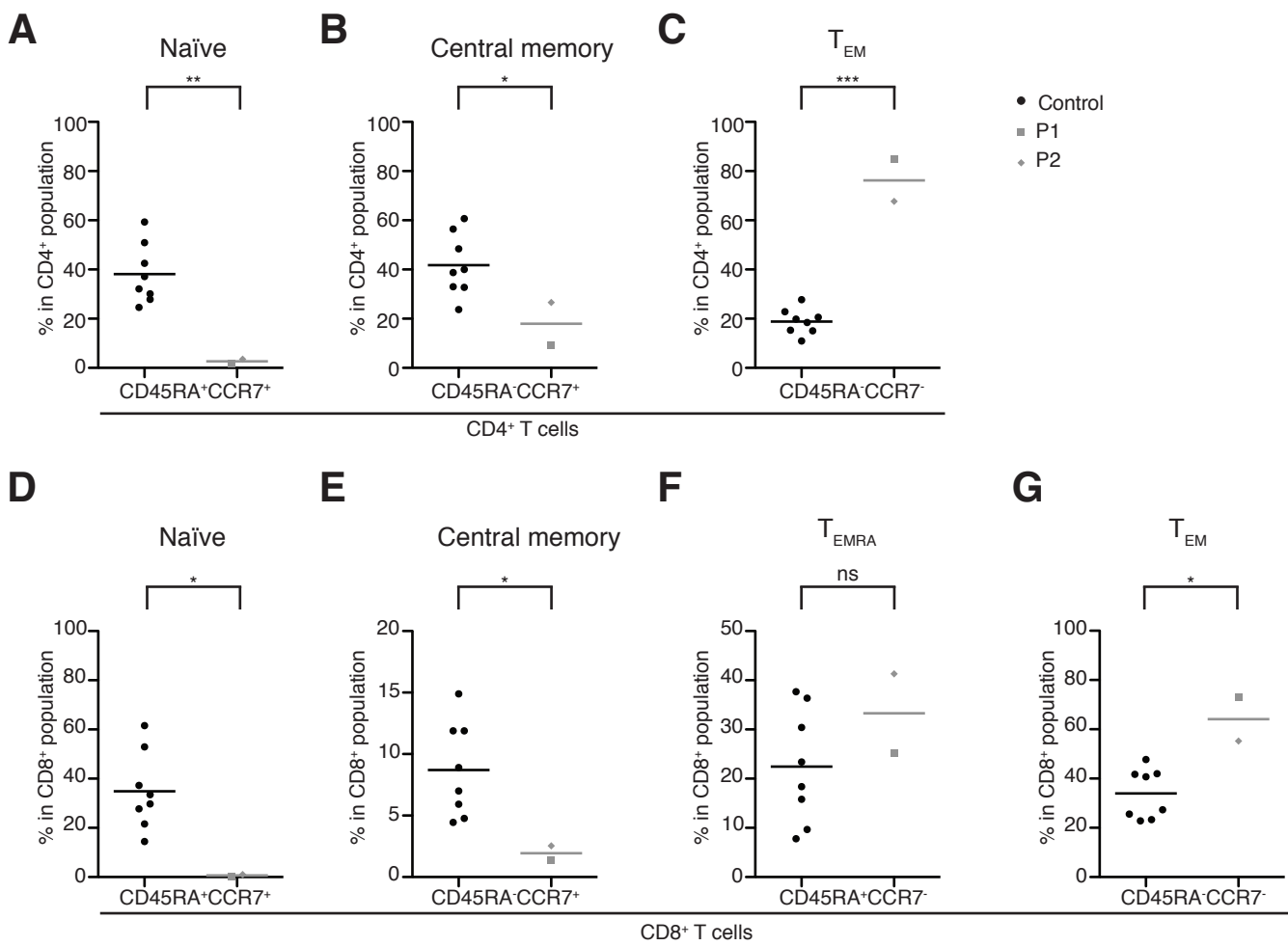
**C**



# Supplemental Figure 3

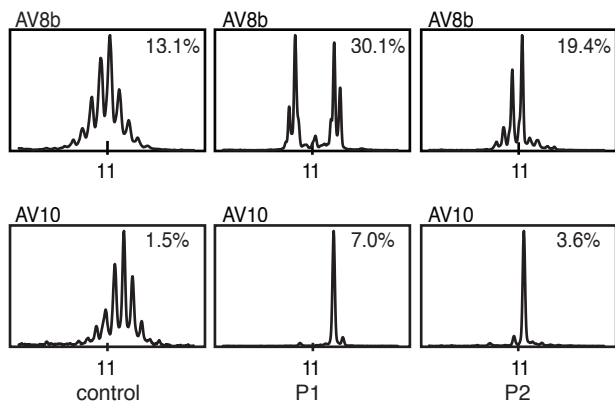
**A****B****C****D****E**

# Supplemental Figure 4

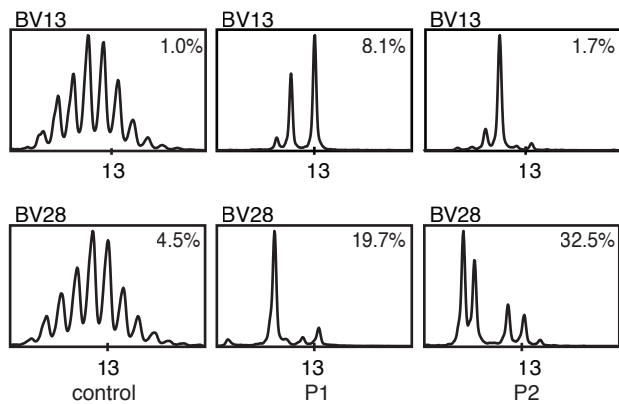


# Supplemental Figure 5

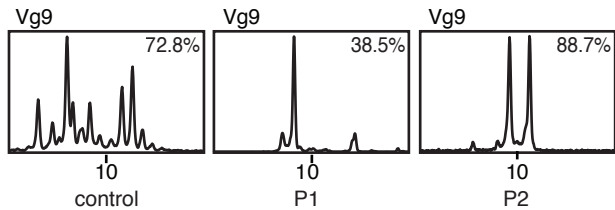
## A



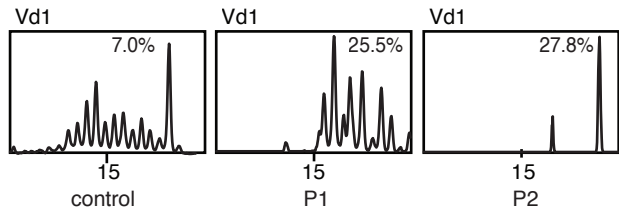
## B



## C



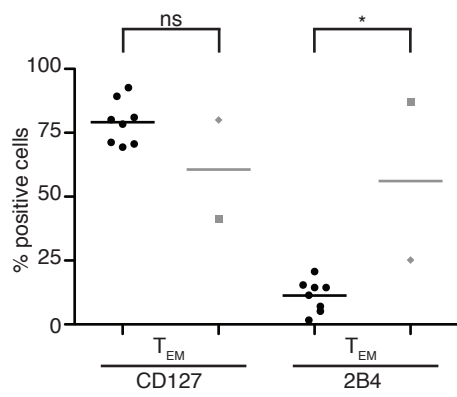
## D



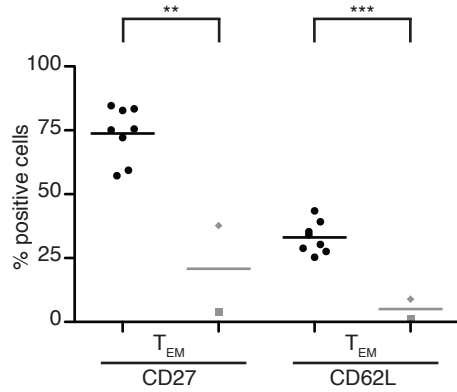
# Supplemental Figure 6

**A**

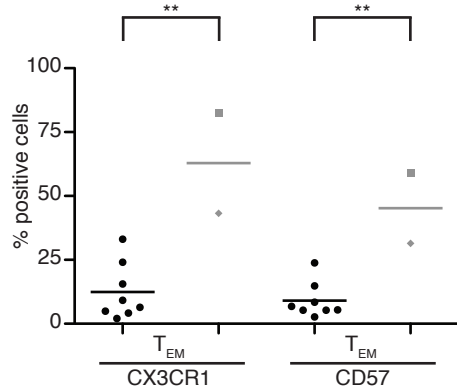
**CD4**



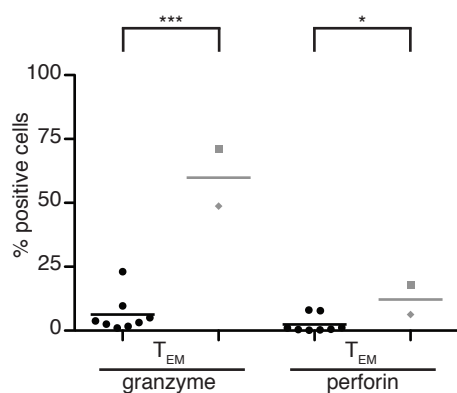
**B**



**C**

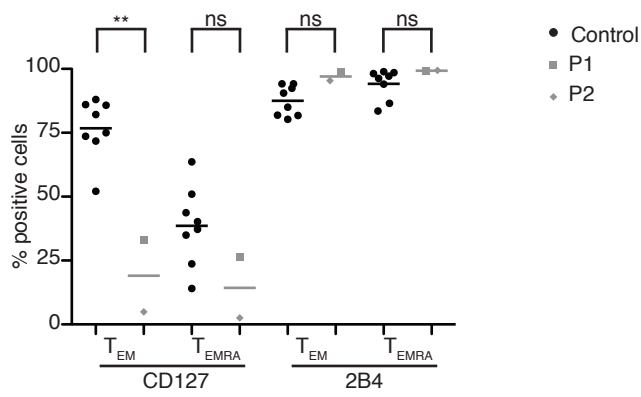


**D**

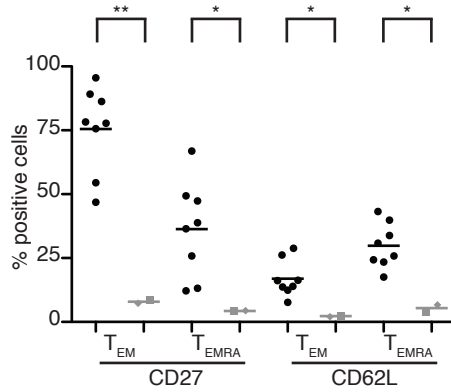


**E**

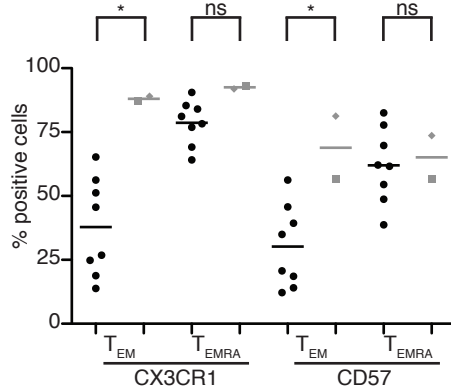
**CD8**



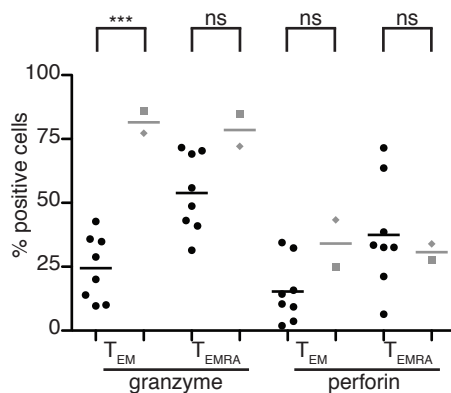
**F**



**G**



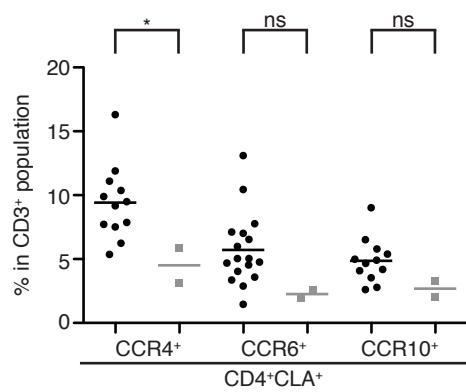
**H**



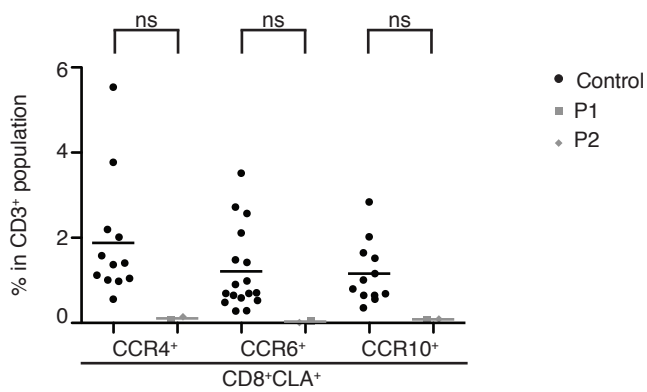
● Control  
■ P1  
◆ P2

# Supplemental Figure 7

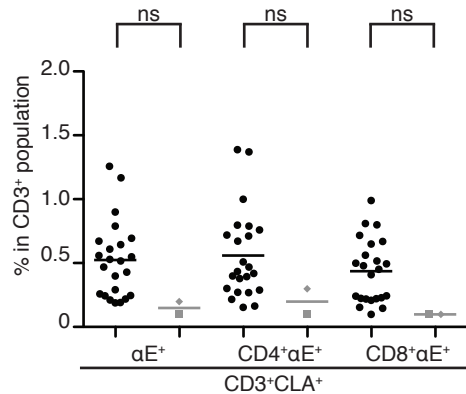
**A**



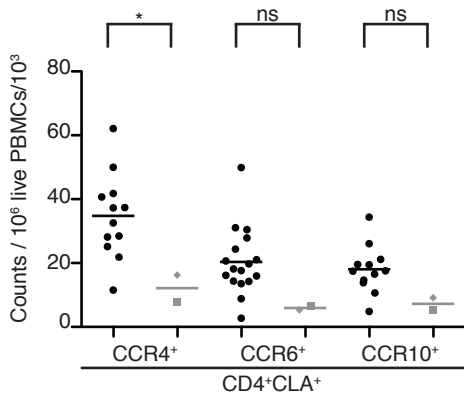
**B**



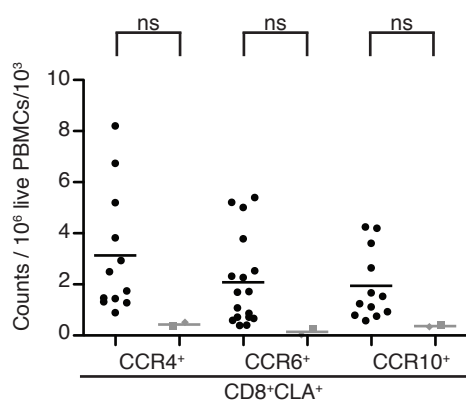
**C**



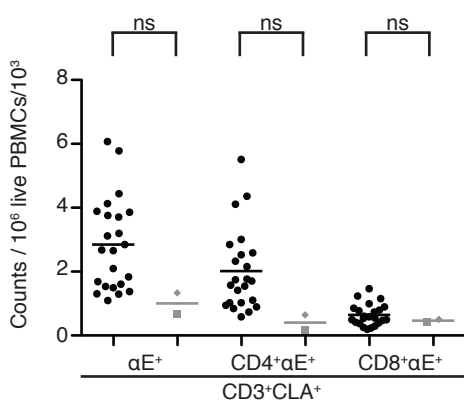
**D**



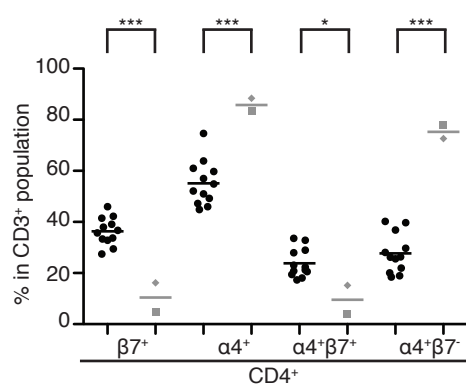
**E**



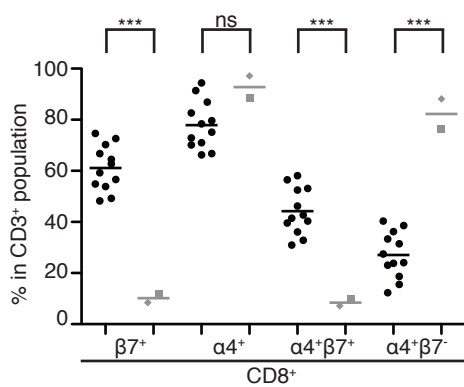
**F**



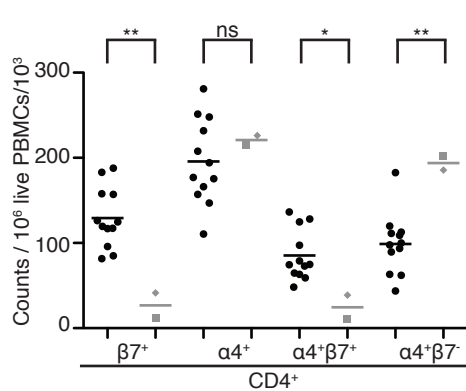
**G**



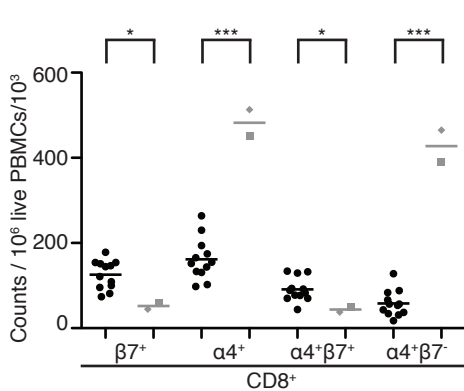
**H**



**I**

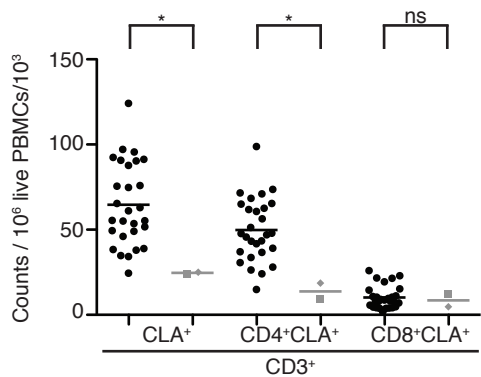


**J**

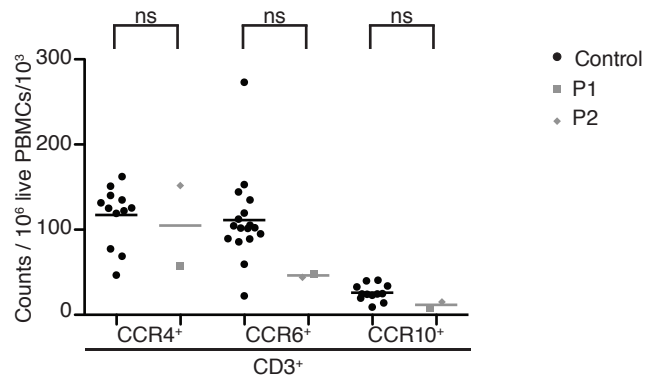


# Supplemental Figure 8

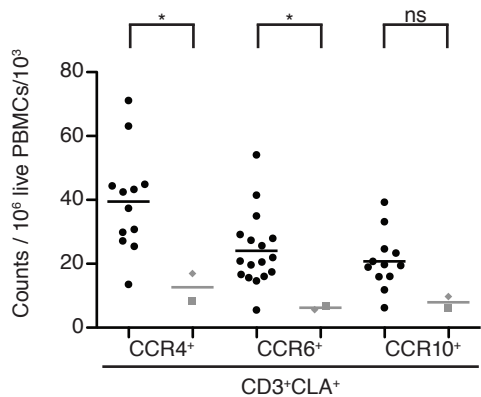
**A**



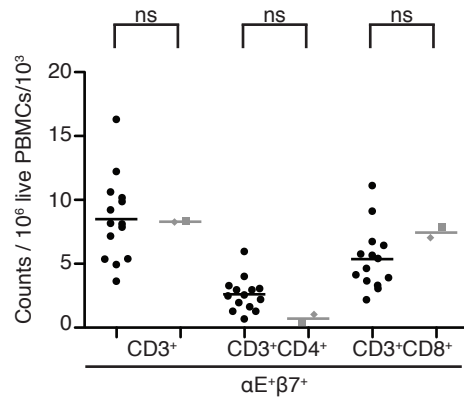
**B**



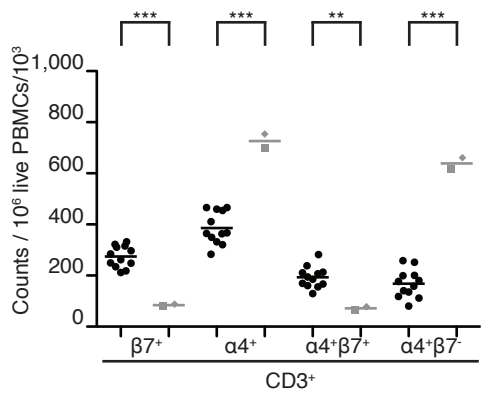
**C**



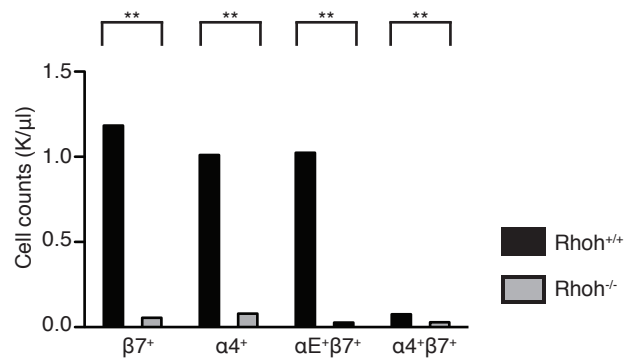
**D**



**E**

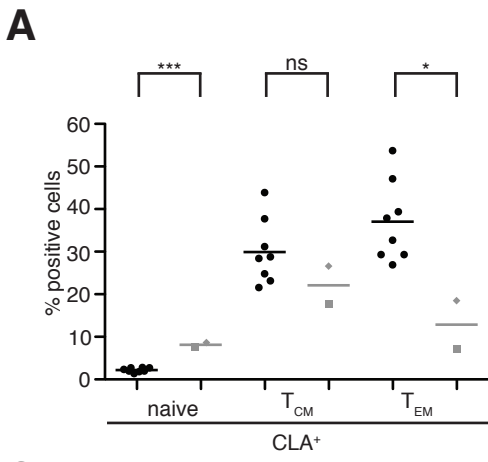


**F**



# Supplemental Figure 9

## CD4<sup>+</sup> cells



## CD8<sup>+</sup> cells

